

## Bulk versus surface effects in normal photoemission from Cu(110) in the range $32 \leq h\nu \leq 160$ eV\*

J. Stöhr,<sup>†</sup> P. S. Wehner, R. S. Williams, G. Apai, and D. A. Shirley

Materials and Molecular Research Division, Lawrence Berkeley Laboratory, Berkeley, California 94720  
and Department of Chemistry, University of California, Berkeley, California 94720

(Received 25 March 1977)

Synchrotron radiation in the 32–160-eV range was used to elucidate the role of bulk and surface effects in normal photoemission from the valence bands of a Cu(110) crystal. A dramatic resonance in the  $s$ - $p$  band was observed for photon energies  $h\nu = 43$ – $52$  eV. We have used this resonance and the energy dependence of the spectra to study the role of surface-induced broadening of the momentum component perpendicular to the surface ( $k_{\perp}$ ). Our results strongly contradict previous interpretations of lower-energy studies in terms of a one-dimensional density of states along  $k_{\parallel}$ . We find that normal photoemission, applied over a sufficient energy range, can be used to map the initial-state bulk band structure.

Recently, Heimann *et al.*<sup>1</sup> studied normal photoemission at  $h\nu = 16.85$  and  $21.22$  eV from (110) faces of Cu, Ag, and Au, and interpreted their results in terms of the *one-dimensional density of states* along the  $\Gamma$ - $K$ - $X$  direction. The apparent lack of conservation of the crystal momentum component perpendicular to the surface ( $k_{\perp}$ ) was attributed to *surface* photoemission from bulk initial states, which extend to the surface, to free-electron-like final states in the vacuum. This result is puzzling because the photoelectron inelastic mean free path in noble metals for electron kinetic energies of  $\sim 20$  eV is typically 10–15 Å.<sup>2</sup> Thus, for normal photoemission from a (110) face about 10 planes contribute and one would expect *bulk* photoemission, characterized by momentum conservation, to be dominant.

In this paper, we report a photoemission study of the (110) face of Cu in the energy range 32–160 eV. The main aim of the present investigation is to elucidate the role of  $k_{\perp}$  in photoemission. Because of the uncertainties associated with  $k_{\perp}$ , most band-structure photoemission studies in the past have been confined to two-dimensional materials.<sup>3</sup> We chose a normal-emission geometry such that  $k_{\parallel} = 0$  and one measures only  $k_{\perp}$ , which is most sensitive to surface-induced effects.<sup>4</sup> Furthermore, for our experimental geometry, the vector potential of the photon field had a large component normal to the surface, and therefore favored surface photoemission.<sup>5</sup>

Our results show that for Cu(110), there exists a definite selection rule on  $k_{\perp}$ , even in the most surface-sensitive energy region. The spectra show a strong photon-energy dependence and differ significantly from the one-dimensional density of states along the  $\Gamma$ - $K$ - $X$  (i.e., the  $k_{\parallel}$ ) direction, in contrast to Ref. 1. All observed peak positions can be accounted for by direct transitions origina-

ting from bulk bands located at well-defined  $\bar{k}$  points in the Brillouin zone (BZ). In their analysis of Cu(001) and Cu(111) spectra,<sup>6</sup> Wagner *et al.*<sup>7</sup> showed that these  $\bar{k}$  points can be determined simply by using a free-electron (empty lattice) band structure for the final state. In Cu(110), a dramatic resonance in the  $s$ - $p$  band just below the Fermi level ( $E_F$ ) for  $43 \leq h\nu \leq 52$  eV can be explained in detail by this model. Thus, the present results strongly support the interpretation of Cu(111) and Cu(100) spectra by Wagner *et al.*<sup>7</sup> and show that at least for Cu, *photon-energy-dependent normal photoemission is a convenient tool for mapping out the initial-state bulk band structure.*

A single crystal of copper with a (110) surface orientation was polished to 1- $\mu$ m smoothness and etched in nitric acid. The surface was cleaned *in situ* by argon-ion bombardment and annealed to remove surface damage. Photoemission measurements were carried out at  $\sim 5 \times 10^{-10}$  Torr in the experimental geometry shown in Fig. 1 of Ref. 6. The crystal was azimuthally oriented such that the surface normal, the [111] and  $[\bar{1}\bar{1}\bar{1}]$  crystalline directions lay in the horizontal plane (see insert in Fig. 2 below). The electron-analyzer resolution was  $\sim 0.2$  eV and the monochromator resolution ranged between 0.01 eV ( $h\nu = 32$  eV) and  $\sim 0.2$  eV ( $h\nu = 160$  eV).

Experimental spectra are shown in Fig. 1. The most striking feature in Fig. 1 is the intense peak, which we shall term Peak A, in the  $s$ - $p$  band region between  $E_F$  and about 2-eV binding energy ( $E_B$ ), which appears for  $43 \leq h\nu \leq 52$  eV. In contrast to previously published Cu spectra<sup>6</sup> peak A is completely new and initially quite surprising. The intensity of this peak is comparable with that of the  $d$ -band peaks in the range  $2 \text{ eV} \leq E_B \leq 5.5$  eV. Also, it shows strong dispersion, ranging from  $E_B = 0.4$  eV at  $h\nu = 43$  eV to  $E_B = 1.7$

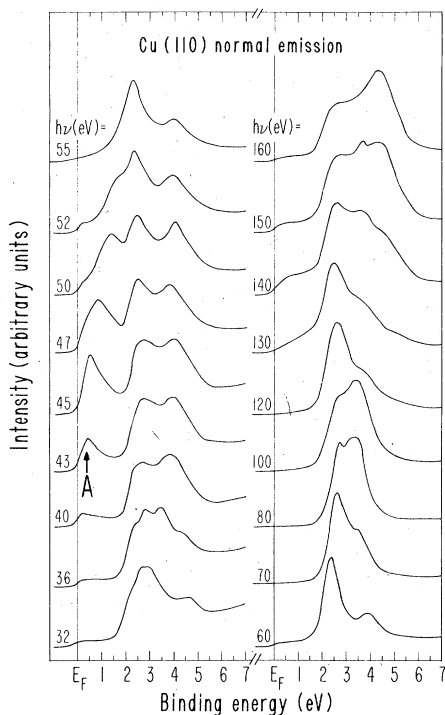


FIG. 1. Photoemission spectra from the valence bands of Cu(110) single crystals in the range  $32 \leq h\nu \leq 160$  eV. Electrons were collected normal to the (110) face with an angular resolution of  $\pm(5 \pm 1)^\circ$ . A is the peak between  $E_F$  and 2 eV in the  $h\nu = 43\text{--}52$  eV spectra.

eV at  $h\nu = 52$  eV. The  $s$ - $p$  intensity vanishes in the energy range  $70 \leq h\nu \leq 120$  eV and shows another maximum around  $h\nu = 140$  eV. At  $h\nu = 160$  eV it has diminished again. The  $d$ -band region also exhibits strong changes in both peak positions and intensities. The  $d$  bandwidth narrows from  $\sim 2.5$  eV (full width at half-maximum (FWHM) at low energies to  $\sim 1.5$  eV in the range  $70 \leq h\nu \leq 120$  eV, then broadens to  $\sim 2.5$  eV at the highest energies.

Figure 2 demonstrates the sensitivity of peak A to the photoemission direction at  $h\nu = 45$  eV. The intensity of peak A decreases greatly at angles  $\theta$  slightly removed from the [110] normal. In particular, for  $\theta = +15^\circ$  it has vanished and the  $s$ - $p$  band shows the expected intensity relative to the  $d$  band.<sup>6</sup> The peak strength varies almost symmetrically on both sides of the normal.<sup>8</sup> Further studies show that peak A is quite insensitive to Ar<sup>+</sup> bombardment of the crystal. Exposure to  $10^3$  L oxygen [1 Langmuir (L) =  $10^{-6}$  Torr sec] reduced its intensity by a factor of 2 relative to the  $d$  band.

The observed peak positions can be related directly to the initial-state band structure as shown in Fig. 3. Figure 3(a) illustrates that for photoemission along the [110] direction the final-state

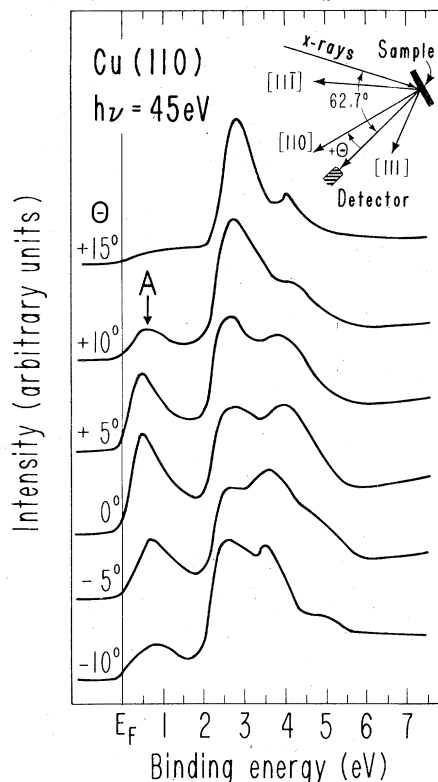


FIG. 2. Dependence of the photoemission spectrum from Cu(110) at  $h\nu = 45$  eV on the polar angle  $\theta$  measured between the sample normal and the photoemission direction into the analyzer.  $\theta$  is defined positive for clockwise rotation of the sample as shown in the insert, negative for counterclockwise rotation.

photoelectron wave vector  $\vec{q}$  in the repeated zone scheme lies along the  $\Gamma$ - $K$ - $X$  direction. By varying the photon energy the endpoint of  $\vec{q}$  will thus sweep through the zone along this line. Figure 3(b) shows Burdick's<sup>9</sup> valence-band structure for Cu along  $UXUKTK$ . Superimposed are the observed peak positions  $E_B(h\nu)$  relative to the Fermi level (cf. Fig. 1). The location of the experimental points in Fig. 3(b) was derived as follows. From the measured peak positions, relative to the Fermi level, the final-state energy  $E_f = E_B(h\nu) + h\nu$  was calculated. The magnitude of the final-state wave vector was then determined from the free-electron dispersion relation  $|\vec{q}| = (2mE_f/\hbar^2)^{1/2}$ , where the zero of the free-electron scale was taken to be the bottom of the free-electron-like bands in Burdick's band structure. The relation  $\vec{q} = \vec{k} + \vec{G}$ , where  $\vec{G}$  is a reciprocal-lattice vector, then yields  $\vec{k}$  in the first BZ and the corresponding values  $E_B(\vec{k})$  are plotted as triangles and bars in Fig. 3(b). Figure 3(c) relates the horizontal scale in Fig. 3(b) to the corresponding photon energy in eV, assuming an initial-state energy of 3.5 eV (middle

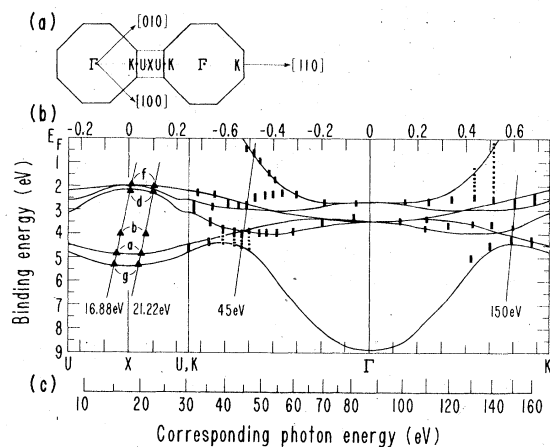


FIG. 3. (a) (001) projection of the three-dimensional Brillouin zone of a fcc lattice in the repeated zone scheme. (b) Burdick's band structure from the Fermi level ( $E_F$ ) to 9 eV binding energy along the UXU and KTK direction in a repeated zone scheme. Filled triangles indicate peak positions of Ref. 1; the bars are the peak positions of Fig. 1. (c) The lower scale establishes a correspondence between the wave vector in Fig. 3(b) and the experimental photon energies as discussed in the text.

of  $d$  band).

Comparison of our experimental peak positions with Burdick's band structure in Fig. 3(b) reveals generally good agreement. One striking result is the complete agreement of the energy dependence of the pronounced  $s$ - $p$  band resonance in Fig. 1 with the dispersion of the uppermost band between K and  $\Gamma$  in Fig. 3(b). In fact, Fig. 3(b) explains why peak A is seen only for  $43 \leq h\nu \leq 52$  eV. In general, the energy dependence of the spectral intensity in the  $E_B$  region  $\leq 2$  eV agrees with the band structure in Fig. 3(b); namely, the intensity is weak below 40 eV, strong around 45 eV, vanishes in the range  $60 \leq h\nu \leq 120$  eV, increases again around 130–140 eV and is weak above 150 eV. The peak positions in the  $d$ -band region  $2 \leq E_B \leq 5.5$  eV also follow Burdick's band structure. For example, the four-peak structure at  $h\nu = 36$  eV corresponds exactly to the band structure near  $k_x = k_y = -0.65$  in Fig. 3(b). The two-peak structure at energies around 80 eV matches the bands close to the  $\Gamma$  point. At  $h\nu = 150$  eV, two wider peaks and a sharp middle peak are observed, in full agreement with the bands at  $k_x = k_y = 0.6$ . Only in the  $E_B$  region 2–3 eV around  $k_x = k_y = -0.4$  do our data points not coincide with Burdick's bands. Here, the discrepancy is about 0.5 eV. It appears unlikely that the experimental peak at  $E_B \sim 2.4$  eV in the corresponding spectra ( $47 \leq h\nu \leq 55$  eV) is caused by transitions from initial states at other  $\vec{k}$  points in the zone, as no flat

bands exist at the respective  $E_B$ . Also, the same discrepancy occurs again at higher photon energies (120–130 eV) corresponding to equivalent  $\vec{k}$  points between  $\Gamma$  and K. This suggests that the initial-state band structure may be in error for these  $\vec{k}$  points.

Figure 3(b) also shows a comparison of the experimental peak positions observed by Heimann *et al.*<sup>1</sup> with Burdick's bands. Because the final states at 16.85 and 21.22 eV lie almost symmetrically around X and the bands are flat around the symmetry point the same experimental peak positions are predicted. We have used the labels of Ref. 1 for the data points in Fig. 3(b). Excellent agreement is found between peaks f, d, a, and g and the band structure. Only peak b, the weakest experimental structure observed, does not coincide with a band around X. The direct-transition model used here predicts the observed peak positions better than the one-dimensional density-of-states (ODDS) calculation of Heimann *et al.* In particular, we need not assume any shift in Burdick's bands to match experimental and theoretically-predicted peak positions, while a 0.3-eV shift had to be assumed by Heimann *et al.* Other discrepancies between the theoretical ODDS of Ref. 1 and experiment lie in the prediction of a shoulder on peak a and especially of the width of peak d. Experimentally, and according to Fig. 3(b) peak d is confined to  $E_B < 2.5$  eV, while the ODDS predict it to extend to  $E_B \sim 3.0$  eV, merging into another peak c at  $E_B = 3.2$  eV, which is not observed experimentally. Thus, with the exception of the weak peak b, the experimental results of Ref. 1 can be accounted for by bulk direct transitions. Weak structures similar to peak b may arise from electrons originating at  $\vec{k}$  points where the bands are flat [e.g.,  $k_x = k_y = -0.4$  in Fig. 3(b)] which reach the detector via scattering at surface irregularities<sup>10</sup> or surface umklapp processes.

In their direct-transition calculation Heimann *et al.* used the model proposed earlier by Christensen and Feuerbacher.<sup>11</sup> In this model, all final states with reduced wave vector  $\vec{k}$  along the  $\Gamma$ -K-X direction are allowed while in our model an additional condition has to be satisfied, namely, that  $\vec{q} = \vec{k} + \vec{G}$  points into the analyzer. The fact that our calculation agrees with experiment thus indicates that the final-state Bloch functions in Cu consist of one strong plane-wave component (i.e., one G vector dominates).

The observed peak intensities, especially that of peak A, require more discussion. A tight-binding linear-combination-of-atomic-orbitals (LCAO) calculation<sup>12</sup> shows the composition of the uppermost band in Fig. 3(b) to be 50%  $s$ - $p$ , 30%  $d_{xy}$ , and 20%  $d_{z^2}$  at  $k_x = k_y = -0.5$ , with its  $d$  character in-

creasing (e.g., 12%  $s-p$ , 47%  $d_{xy}$ , and 41%  $d_{z^2}$  at  $k_x = k_y = -0.375$ ) as the band moves away from the Fermi energy. The amount of  $d$ -like character of this band can explain the strength and angular dependence of peak A. An LCAO calculation shows that, while its energy remains almost unchanged, the orbital character of the uppermost band in Fig. 3(b) changes drastically for  $\vec{k}$  points off the  $\Gamma$ - $K$  symmetry line. In fact, for  $\vec{k}$  points corresponding to  $h\nu = 45$  eV and an emission angle  $\phi$  as defined in Fig. 2 the composition of this band changes from 42%  $s-p$ , 35%  $d_{xy}$ , 23%  $d_{z^2}$  for  $\theta = 0^\circ$ , to 84%  $s-p$ , 10%  $d_{xy}$ , 6%  $d_{z^2}$  for  $\theta = 10^\circ$  to almost pure  $s-p$  (95%) character for  $\theta = 15^\circ$ . The strong  $s-p$  character (e.g., 87%  $s-p$  for  $k_x = k_y = -0.375$ ) of the lowest band in Fig. 3 is also the reason why it is not observed experimentally.

Peak A does not reappear in the region  $130 \leq h\nu \leq 140$  eV as one would expect from Fig. 3. Besides sampling larger  $k_{||}$  values at higher energies due to the finite angular resolution of the analyzer

we attribute this mainly to a shorter inelastic mean free path  $\Lambda_e$  around 130–140 eV ( $\Lambda_e \approx 3 \text{ \AA}$ ) than around 45 eV ( $\Lambda_e \approx 8 \text{ \AA}$ ),<sup>2</sup> resulting in a larger broadening of  $k_{\perp}$ .<sup>4</sup> We can estimate an upper limit for this broadening at  $h\nu = 45$  eV from the width (0.9 eV) of peak A taking the experimental resolution (0.2 eV) into account. This yields  $\Delta k_{\perp} \approx \pm 0.035$  ( $2\pi/a$ ), where  $a$  is the Cu lattice constant. With the above values for  $\Lambda_e$  we obtain  $\Delta k_{\perp} \approx \pm 0.1$  ( $2\pi/a$ ) for  $130 \leq h\nu \leq 140$  eV. While this value for  $\Delta k_{\perp}$  is sufficient to smear out the sharp structure of peak A we note that it is only 10% of the Brillouin-zone dimension. Thus from these estimates Cu(110) photoemission spectra are not expected to resemble a one-dimensional density of states along  $k_{\perp}$  even in the region of highest surface sensitivity, in gross disagreement with Ref. 1. Finally we mention that the present results on Cu also contrast with the interpretation of PbS photoemission spectra which were recently published by Grandke *et al.*<sup>13</sup>

<sup>†</sup>Present address: Stanford Synchrotron Radiation Laboratory, Stanford, Calif. 94305.

\*Work performed at the Stanford Synchrotron Radiation Project, which is supported by the NSF Grant No. DMR 73-07692 A02, in cooperation with the Stanford Linear Accelerator Center and was done with support from the U. S. ERDA.

<sup>1</sup>P. Heimann, H. Neddermeyer, and H. F. Roloff, *Phys. Rev. Lett.* **37**, 775 (1976).

<sup>2</sup>I. Lindau and W. E. Spicer, *J. Electron Spectrosc.* **3**, 409 (1974); C. R. Brundle, *Surf. Sci.* **48**, 99 (1975); I. Lindau, P. Pianetta, K. Y. Yu, and W. E. Spicer, *J. Electron Spectrosc.* **8**, 487 (1976); D. T. Ling (private communication) found the escape depth for Cu(110) to be shortest around 80 eV.

<sup>3</sup>See, for example, N. V. Smith and M. M. Traum, *Phys. Rev. B* **11**, 2087 (1975).

<sup>4</sup>P. J. Feibelman and D. E. Eastman, *Phys. Rev. B* **10**, 4932 (1974).

<sup>5</sup>G. D. Mahan, *Phys. Rev. B* **2**, 4334 (1970); W. L. Schaich and N. W. Ashcroft, *ibid.* **3**, 2452 (1971).

<sup>6</sup>J. Stöhr, G. Apai, P. S. Wehner, F. R. McFeely, R. S. Williams, and D. A. Shirley, *Phys. Rev. B* **14**, 5144 (1976).

<sup>7</sup>L. F. Wagner, Z. Hussain, and C. S. Fadley, *Solid State Commun.* **21**, 257 (1977).

<sup>8</sup>Note that the  $d$ -band peaks are not symmetrical about  $\theta = 0^\circ$ . This is probably due to the different orientation of the  $\vec{E}$  vector with respect to the crystalline axes for positive and negative  $\theta$  (cf. Ref. 10).

<sup>9</sup>G. A. Burdick, *Phys. Rev.* **129**, 138 (1963).

<sup>10</sup>E. Dietz, H. Becker, and U. Gerhardt, *Phys. Rev. Lett.* **36**, 1397 (1976).

<sup>11</sup>N. E. Christensen and B. Feuerbacher, *Phys. Rev. B* **10**, 2349 (1974).

<sup>12</sup>We have used the N. V. Smith [*Phys. Rev. B* **3**, 1862 (1971)] parametrization of the L. Hodges, H. Ehrenreich, and N. D. Lang [*Phys. Rev.* **152**, 505 (1966)] LCAO interpolation scheme.

<sup>13</sup>T. Grandke, L. Ley, and M. Cardona, *Phys. Rev. Lett.* **38**, 1033 (1977).